SCIENCE CHINA
Earth Sciences

•RESEARCH PAPER•

August 2022 Vol.65 No.8: 1477–1489
https://doi.org/10.1007/s11430-021-9916-1

Overlooked contribution of the biological pump to the Pacific Arctic nitrogen deficit

Hongliang LI[1], Jianfang CHEN[1,2*], Diana RUIZ-PINO[3], Jingjing ZHANG[1,4], Haiyan JIN[1], Yanpei ZHUANG[5], Youcheng BAI[1], Jian REN[1] & Yangjie LI[1]

[1] *Key Laboratory of Marine Ecosystem Dynamics, Second Institute of Oceanography, Ministry of Natural Resources, Hangzhou 310012, China;*
[2] *State Key Laboratory of Satellite Ocean Environment Dynamics, Hangzhou 310012, China;*
[3] *Sorbonne Universités (UPMC, Université Paris 06)-CNRS-IRD-MNHN, LOCEAN Laboratory, 4 Place Jussieu, Paris F-75005, France;*
[4] *Southern Marine Science and Engineering Guangdong Laboratory (Zhuhai), Zhuhai 519080, China;*
[5] *Polar and Marine Research Institute, Jimei University, Xiamen 361021, China*

Received September 27, 2021; revised February 26, 2022; accepted March 2, 2022; published online July 6, 2022

Abstract The nutrient-rich Pacific Ocean seawater that flows through the Bering Strait into the Chukchi Sea is generally considered to be the most important source of nutrients to the Arctic euphotic zone. The inflow is characterized by nitrogen deficit and low nitrate/phosphate (N/P) ratios; this is ascribed to sedimentary denitrification on the Chukchi shelf by preoccupant opinions. However, the Chukchi Sea also has high primary production, which raises the question of whether the biological pump may also significantly modulate nutrient properties of the throughflow. Here, we show that nitrate concentrations of the Pacific inflow gradually decrease northward in association with notable biological utilization. The phytoplankton N/P uptake ratio was 8.8±2.27, higher than the N/P ratio of Pacific inflow water (5–6). This uptake ratio, in combination with efficient vertical nitrogen export, serves to preferentially remove nitrogen (relative to phosphorus) from upper waters, thereby further intensifying the Arctic nitrogen deficit. Accordingly, as large as about 111.7×10^9 mol N yr^{-1} of nitrate was extra consumed, according to the real N/P uptake ratio rather than the ratio of the Pacific inflow, which may be as great as half the nitrogen loss ascribed to sedimentary denitrification. Our findings suggest that besides sedimentary denitrification, biological disproportionate utilization of nutrients in the Chukchi Sea upper water is another important contributor to the nitrogen limitation and excess phosphorus in the upper Arctic Ocean. In the rapid Arctic change era, the predicted reinforced biological carbon pump could further impact the nutrient dynamics and biogeochemical process of the Arctic Ocean.

Keywords Nitrogen deficit, Biological pump, Nutrient, Sinking particles, Arctic Ocean

Citation: Li H, Chen J, Ruiz-pino D, Zhang J, Jin H, Zhuang Y, Bai Y, Ren J, Li Y. 2022. Overlooked contribution of the biological pump to the Pacific Arctic nitrogen deficit. Science China Earth Sciences, 65(8): 1477–1489, https://doi.org/10.1007/s11430-021-9916-1

1. Introduction

The role of nitrogen availability in Arctic Ocean biogeochemical processes is a subject of much interest and speculation (Codispoti et al., 2005, 2009; Brown et al., 2015; Tremblay et al., 2015)—particularly so because of the polar ocean's general condition of nitrogen (N) limitation, its strategic role as a conduit connecting the Pacific and Atlantic oceans, its importance in regulating the global oceanic N budget (Yamamoto-Kawai et al., 2006), and the general scarcity of field observations of Arctic biogeochemical quantities. Because the Arctic Ocean is almost entirely surrounded by continents (Eurasia and North America), its major source of nutrients is advective input from the Pacific

* Corresponding author (email: jfchen@sio.org.cn)

and Atlantic oceans (Walsh et al., 1989; Torres-Valdés et al., 2013).

Historically, the volume of Pacific inflow, which arrives via the Bering Strait (Figure 1), has been only about one-tenth the volume of Atlantic inflow (Beszczynska-Möller et al., 2011; Woodgate, 2018). Nevertheless, the biological impact of the Pacific water rivals that of the Atlantic water. The Pacific inflow is relatively warm and of low salinity and therefore low in density. As a result, this water is confined to upper (e.g., sunlit) layers hospitable for photosynthetic activity (McLaughlin et al., 2004; Woodgate, 2018). In addition, N input through the Bering Strait (upper 50 m) is almost 20 times greater than that arriving through Atlantic gateways (Torres-Valdés et al., 2013). In short, Pacific inflow constitutes the largest horizontal source of N to the Arctic Ocean and thus plays an important role in stimulating high-latitude biological activity.

As the Pacific inflow water travels northward across the Chukchi shelf (Figure 1), its chemical properties are modified by local biogeochemical processes (Devol et al., 1997; Cooper et al., 1999; Chang and Devol, 2009; Brown et al., 2015). Notably, coupled sedimentary nitrification-denitrification in the Chukchi Sea leads to a fixed N loss of about 3.0 Tg N yr^{-1}, which is about 1–3% of the world ocean total (Chang and Devol, 2009). As a result, the seawater nitrate/phosphate (N/P) ratio drops to extremely low values (e.g., 3.6 in the northern Chukchi Sea), even during the winter (pre-bloom) period (Tremblay et al., 2015). Transpolar transport of the resulting excess P goes on to fuel dinitrogen (N_2) fixation in the North Atlantic Ocean (Yamamoto-Kawai et al., 2006).

The Bering-Chukchi shelf is one of the world ocean's most productive areas (Grebmeier et al., 2015; Hill et al., 2018), and this biological activity also modifies the nutrient content of the Pacific throughflow water. Through photosynthesis, the incorporation of seawater nutrients into cellular tissue, and then the sedimentation of some fraction of that organic matter (i.e., the action of the "biological pump"), the concentrations of seawater nutrients are gradually reduced during the Chukchi Sea transit (Codispoti et al., 2005, 2009). Recently, the phytoplankton N/P utilization ratio over the Chukchi shelf was documented to be lower than the canonical Redfield ratio (Mills et al., 2015), thus indicating that not only nutrient concentrations and loads but also relative proportions are being modified within the Chukchi Sea.

To date, however, there has been a little systematic study of the effects of the Chukchi biological pump on the properties of Pacific water entering the Arctic via the Bering Strait gateway. Interest in quantifying such effects is motivated additionally by the many rapid changes now occurring in the Arctic and in the Chukchi Sea in particular. In recent years, for example, the Pacific inflow volume has increased dramatically (38%–67% increase between 1990 and 2015) (Woodgate, 2018), as has annual net primary production in the Chukchi Sea (42% increase between 1998 and 2012) (Arrigo and van Dijken, 2015).

We, therefore, analyzed properties of the Chukchi Sea waters, suspended and sinking particles, and surface sediments (measured in 2003 and 2008–2009) in order to quantify modification of the inflowing Pacific water by biological activity. Specifically, we used stable N isotope data from surface sediments and particles together with hydrographic and biogeochemical data (e.g., salinity, temperature, and nutrient and chlorophyll-*a* concentrations) to assess biological N utilization over a range of spatial and temporal scales, quantify vertical N export from upper waters, and characterize changes in seawater nutrient structure (i.e., N/P ratios) over the course of the Chukchi Sea transit.

2. Materials and methods

Two Chinese National Arctic Research Expedition (CHINARE) cruises were conducted on the icebreaker Xuelong (2003 and 2008) to cover the northern Bering shelf, Chukchi Sea, and Canada Basin (Figure 1). During the 2003 cruise (31 July through 8 September), surface sediment samples (0–2 cm depth) were collected with a 0.64 m^2 box corer at 14 stations in water depths ranging from 50 to 100 m. During the 2008 cruise (1 August through 8 September), discrete seawater samples were collected at 41 stations located in water depths ranging from 50 to 2000 m. Niskin bottles (12 l each) were mounted onto a rosette sampling assembly, and seawater was collected from the upper water column (at 2, 10, 20, 30, 50, 75, and 100 m). Samples were also collected at a depth of the chlorophyll-*a* maximum and at the sea bottom (i.e., 2 m above the seafloor). Continuous vertical profiles of standard hydrographic data were collected as well. From 7 August 2008 to 30 September 2009, a time-series sediment trap was moored at station M01 (158.23°W, 74.40°N) on the Chukchi slope. The water depth at this station is 1650 m, and the depth of the sediment trap was 870 m.

A Mark 78H-21 time-series sediment trap (McLane, USA) was used to collect sinking particles at station M01 (Figure 1). The trap had 21 collection bottles, a collection area of 0.5 m^2, and a sample collection interval of 15–31 days. This interval was adjusted seasonally according to the typical seasonal cycle of primary production, with samples being collected more frequently during the warm season. Before trap deployment, the 500 mL polyethylene bottles were filled with trap-depth filtered seawater. Analytical grade NaCl (35 g L^{-1}) and $HgCl_2$ (3.3 g L^{-1}) were added to the bottles to minimize diffusion and inhibit bacterial degradation of the samples. After trap recovery, the wet samples were passed through a 1 mm mesh nylon sieve to remove zooplankton and checked by microscopy (Knap et al., 1996). The <1 mm fractions were then split into five equal aliquots by a high-precision rotary

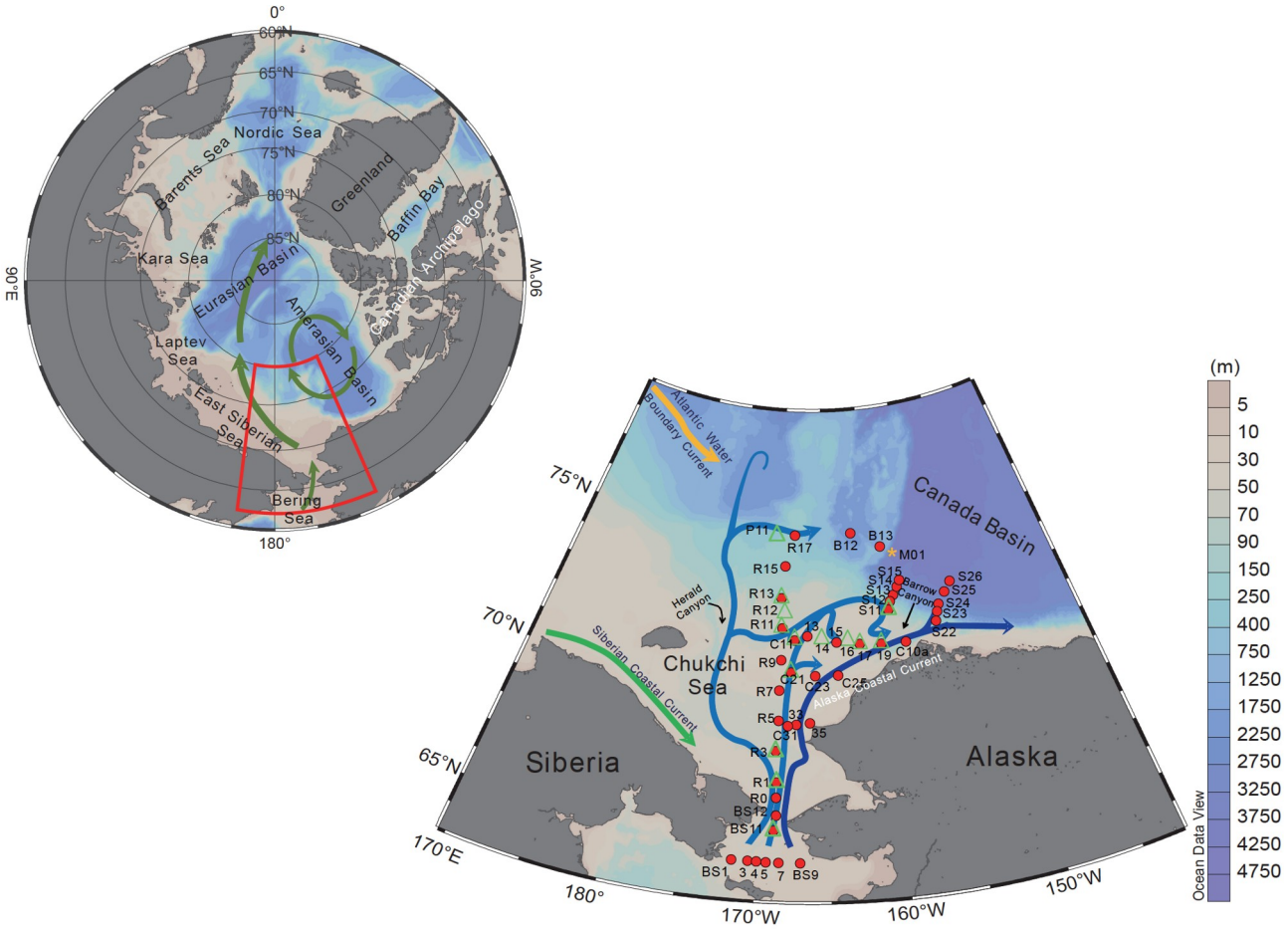

Figure 1 Bathymetric chart of the Chukchi Sea, showing general flow paths of water from the Pacific Ocean into the Arctic Ocean (modified from Itoh et al., 2015). The green triangles mark station locations where surface sediments were sampled (July–September 2003), and the red dots mark stations where water column nutrients and suspended particles were sampled (July–September 2008). The yellow asterisk marks where sediment trap M01 was moored (August 2008–September 2009).

splitter (McLane WSD-10), and each sample split was filtered onto a pre-weighed polycarbonate filter (0.45 μm pore size). Finally, the samples were dried at 45°C for 72 h and then weighed for measurements of total particle flux.

Surface sediments and water-column suspended particulates were both analyzed for stable isotopes of nitrogen (δ^{15}N). The box-core samples were initially stored at −20°C for later processing. The suspended particulate nitrogen (PN) samples were obtained by filtering 4 l of seawater through pre-weighed, pre-combusted (450°C for 4 h) Whatman GF/F filters (47 mm diameter, 0.7 μm pore size). The filters were then wrapped in pre-combusted aluminum foil and stored at −20°C for later processing. Prior to the isotope analyses, the surface sediments and PN filter samples were freeze-dried. The sediments were ground in an agate mortar, and depending on the content of organic material in the samples, part of the PN filter samples were packed in tin foil directly for isotope analysis. Measurements of the stable N isotope ratio of the surface sediments ($\delta^{15}N_{sediment}$) and the PN samples (δ^{15}PN) were carried out using a Carlo Erba elemental analyzer interfaced via a ConFlo II to a Finnigan Delta Plus mass spectrometer. The N isotopic data are presented in the conventional δ notation with respect to the standard of atmospheric nitrogen. The analytical precision of the δ^{15}N measurements (as determined from replicate analyses) was ±0.3‰.

The seawater samples were analyzed for concentrations of nitrate ($[NO_3^-]$), nitrite ($[NO_2^-]$), and phosphate ($[PO_4^{3-}]$) (where square brackets denote concentrations), as well as chlorophyll-*a* ([Chl-*a*]). The nutrient samples were filtered through cellulose acetate membranes (47 mm diameter, 0.45 μm pore size), and the filtrate was analyzed on board the ship with a continuous flow injection analyzer (Skalar san++, Holland, Breda) and the colorimetric methods described by Grasshoff et al. (1999). For the measurements of $[NO_3^- + NO_2^-]$ and $[NO_2^-]$, the precision was 1% and the detection limit was 0.1 μmol L^{-1}; for $[PO_4^{3-}]$, the precision was 2% and the detection limit was 0.03 μmol L^{-1}. The value of

$[NO_3^-]$ was calculated as the difference between $[NO_3^- + NO_2^-]$ and $[NO_2^-]$. The nutrient values were salinity corrected. The Chl-*a* samples (250 mL of seawater each) were filtered through Whatman GF/F filters (25 mm diameter, 0.7 μm pore size). The filter samples were then analyzed according to the fluorometric acidification procedure described in Holm-Hansen et al. (1965). At each station, vertical profiles of salinity (*S*) and temperature (*T*) were recorded with a Seabird (model SBE 911 plus) conductivity-temperature-depth (CTD) recorder (General Oceanic, USA).

The quantities of seasonal $[NO_3^-]$ and $[PO_4^{3-}]$ drawdowns were estimated from changes in their depth-integrated concentrations (0 to 100 m)—i.e., differences between the pre-growing season concentrations (assumed) and our sampling-period concentrations (measured) (as in Mills et al., 2015). The phytoplankton N/P utilization ratio was then calculated as the ratio of these two seasonal differences (deficits). Initial nutrient concentrations (prior to the spring bloom) were assumed to be equal to the mean Pacific winter water (PWW) concentrations measured on the Chukchi shelf during the 2008 cruise. The N^{**} is determined as follows: $N^{**}=([NO_3^-]+[NO_2^-])-8.8\times[PO_4^{3-}]+2.98)$, a non-Redfield N/P ratio (8.8) was used in the equation. This non-Redfield N/P ratio (8.8) was calculated according to seasonal nutrients deficit, which represented the real nutrient uptake ratio of the phytoplankton in the study area (details in discussion 4.3).

We also examined environmental parameters for the M01 sediment trap station (Figure 1) for the period July 2008 to September 2009. National Oceanic and Atmospheric Administration (NOAA) Daily Optimum Interpolation Sea Surface Temperature (SST) data, 1/4° spatial resolution, were taken from http://apdrc.soest.hawaii.edu/dods/public_data/NOAA_SST/OISST_AVHRR_AMSR. Biweekly sea ice concentration data were provided by the National Snow and Ice Data Center (NSIDC), with grid cell dimensions of 25 km×25 km: http://nsidc.org/data/NSIDC-0051. Solar 8-day Photosynthetically Active Radiation (PAR) data were obtained from the National Aeronautics and Space Administration (NASA) Moderate Resolution Imaging Spectroradiometer (MODIS), with a horizontal resolution of 4 km: https://giovanni.gsfc.nasa.gov/giovanni.

3. Results

3.1 Hydrographic conditions

The complex hydrography of the Chukchi shelf during the August 2008 cruise can be seen in the relationship between potential temperature (θ) and S shown in Figure 2. The Pacific-origin waters on the Chukchi shelf could be generally separated into summer water and winter water. The summer water consisted of warm and fresh Alaska Coastal Water (ACW) and cooler and saltier summertime Bering Sea Water (BSW) (e.g., Steele et al., 2004). The winter water consisted of cold, relatively saline PWW (e.g., Weingartner et al., 2005). The warmest ACW was characterized by $T>3$°C and $S<32$, with oligotrophic $[NO_3^-]$ (i.e., $[NO_3^-]<0.5$ μmol L^{-1}). At station C35, the station nearest the Alaska coast (Figure 1), surface water *T* was 6.91°C and *S* was 27.68. The BSW water mass was identifiable by its intermediate temperature ($-1<T<3$°C) and salinity ($30<S<32.8$). The coldest water was PWW, distinguishable by its low temperature ($T<-1$°C), high salinity ($31.5<S<33.6$), and the highest $[NO_3^-]$ encountered on the cruise (>10 μmol L^{-1}, Figure 2a). During the warm season, the melting of sea ice forms a thin layer of fresh water at the sea surface. This ice melt water (IMW) was characterized by low salinity ($S<30$) and a wide temperature range ($-1<T<6$°C).

Figure 2b showed that the N/P ratios of the different water masses on the Chukchi Shelf were generally <8.0 during the 2008 summer cruise. The overall highest ratios were observed in the PWW, with a range of 4.8 to 6.9 and an average of 5.7±0.42.

3.2 Nutrient and Chl-*a* distributions

Figure 3a and 3b show the spatial distribution of $[NO_3^-]$ in surface and bottom waters. In surface waters, $[NO_3^-]$ generally hovered near the detection limit: 1.43±3.21 μmol L^{-1} on average, ranging from 0.10 to 16.0 μmol L^{-1}. A few high-$[NO_3^-]$ exceptions were encountered in low-T, high-S samples from the western Bering Shelf and Bering Strait. At bottom depths, $[NO_3^-]$ values were much higher: 8.39±4.87 μmol L^{-1} on average, ranging from 0.17 to 16.1 μmol L^{-1}. At several stations on the eastern shelf, low $[NO_3^-]$ was found in both surface and bottom waters due to the influence of oligotrophic ACW. The highest concentrations (>10 μmol L^{-1}) occurred in a patch of PWW on the central Chukchi shelf. The mean PWW concentration of 12.2±1.5 μmol L^{-1} was assumed to be representative of the pre–growing season concentration (Table 1).

The regional distribution of $[PO_4^{3-}]$ (Figure 3c–3d) was similar to that of $[NO_3^-]$: where $[NO_3^-]$ was high, so was $[PO_4^{3-}]$. In surface waters, the average $[PO_4^{3-}]$ was 0.70±0.37 μmol L^{-1} and the range was 0.21 to 2.08 μmol L^{-1}. At bottom depths, the average was 1.58±0.53 μmol L^{-1} and the range was 0.53 to 2.20 μmol L^{-1}. The mean PWW concentration of 2.10±0.19 μmol L^{-1} was assumed to be representative of the pre–growing season concentration (Table 1).

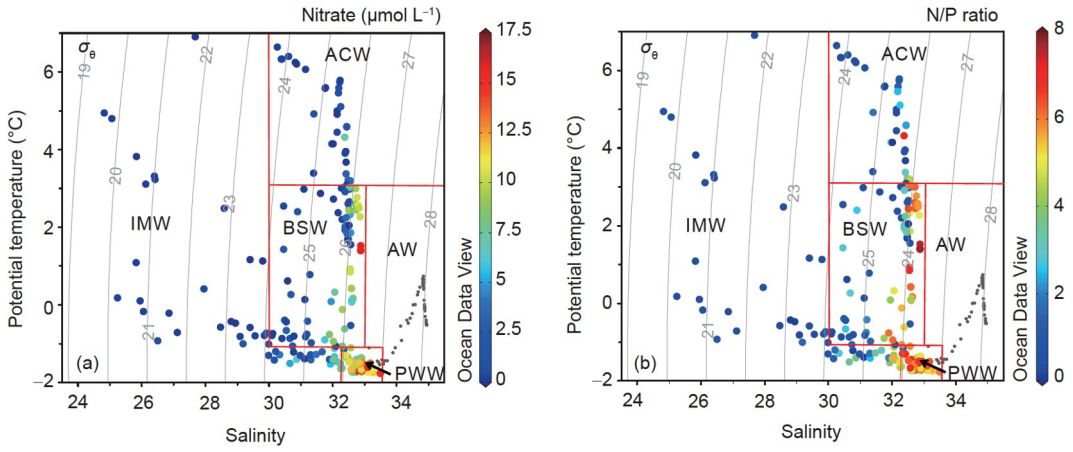

Figure 2 Characteristics of Chukchi Sea water masses, August–September 2008: θ–S diagrams with isopycnal lines of potential density (σ_θ) and data point colors indicating (a) $[NO_3^-]$ and (b) N/P ratios. The rectangular outlines indicate the properties of the water masses considered in this study: IMW, Ice Melt Water; ACW, Alaska Coastal Water; BSW, Bering Shelf Water; PWW, Pacific Winter Water; AW, Atlantic Water (sampled but not used in this study).

Table 1 Nutrient parameters measured in 25 samples of Pacific winter water during the CHINARE 2008 cruise

	Mean±SD (μmol L^{-1})	Maximum (μmol L^{-1})
$[NO_3^-]$	12.2±1.5	15.3
$[PO_4^{3-}]$	2.1±0.19	2.5
N/P	5.7±0.42	6.9

Concentrations of Chl-*a* were showed in Figure 3e–3g. In surface layer, the [Chl-*a*] ranged from 0.03 to 22.41 mg m^{-3}, with an average of 2.97±5.32 mg m^{-3} (Figure 3e). Patches of high [Chl-*a*] were encountered on the central Bering shelf (~15 mg m^{-3}), in the Bering Strait (20 to 23 mg m^{-3}), and in the central-shelf area of PWW influence (5 to 10 mg m^{-3}). At bottom depths (Figure 3f), high [Chl-*a*] was found in the areas with high-chlorophyll surface patches, in the Bering Strait, and in the area of PWW influence. Average bottom-depth [Chl-*a*] was 1.87±1.83 mg m^{-3}, with a range of 0.04 to 6.80 mg m^{-3}.

Figure 4 showedvertical sections across the Chukchi Sea (meridional section R) and the Bering Strait (zonal section BS) (Figure 1). On the Chukchi shelf, the macronutrients NO_3^- and PO_4^{3-} exhibited the pronounced vertical gradients typical of summertime conditions (Figure 4c, 4d). Nitrate above the base of the mixed layer (i.e., approximately the upper 5 to 30 m, Coupel et al., 2015) was generally depleted except in the Bering Strait and adjacent southern Chukchi shelf (approximately 65°N to 68°N). At depth, $[NO_3^-]$ was much greater, especially in the northern shelf waters (72°N to 75°N), which originated from PWW (low T, high S). Phosphate distributions were similar to those of nitrate but at replete levels (i.e., >0.5 μmol L^{-1}).

The vertical section of [Chl-*a*] across the Chukchi shelf (Figure 4e) showed notable latitudinal and vertical gradients. High [Chl-*a*] occurred in the Bering Strait, with a gradual decrease northward. As with $[NO_3^-]$ and $[PO_4^{3-}]$, the depth of maximum [Chl-*a*] deepened from surface waters in the Bering Strait to subsurface waters (i.e., ~30 m) on the northern shelf.

3.3 δ^{15}N Distributions and temporal variability

3.3.1 Latitudinal gradients of δ^{15}N in suspended particulates and surface sediments

Values of δ^{15}PN in suspended particulates generally increased poleward. In surface waters (Figure 5a), δ^{15}PN ranged from 5.4‰ to 8.9‰, with an average of 7.0‰±1.0‰. The lightest values (5.4‰ to 5.7‰) were encountered on the northern Bering shelf, with increases to approximately 7.0‰ along the pathway of water transport toward the southern Chukchi shelf. Over the Chukchi shelf, values were notably lowest in southern areas, with the richest values (7.3‰ to 8.8‰) encountered on the northern shelf. The maximum value (8.9‰) occurred just off the northern coast of Alaska. In bottom waters (Figure 5b), the pattern of δ^{15}PN distribution was generally similar to that of surface waters. Values ranged from 5.6‰ to 10.2‰, with an average of 7.2‰±1.3‰.

Figure 4f showed the vertical distribution of δ^{15}PN of suspended particles along transect *R* (170°W), from the Bering Strait to the northern Chukchi shelf. Mixed-layer δ^{15}PN generally increased northward along the path of water flow, from about 5.5‰ at 65.5°N in the Bering Strait to about 10.0‰ at 75°N. The depth of δ^{15}PN enrichment (i.e., maximum δ^{15}PN) gradually increased (deepened) northward as well. Beneath the mixed layer (i.e., about 5 to 30 m, Coupel et al., 2015), values of δ^{15}PN were relatively light (ranging from 5.0‰ to 7.0‰) from the Bering Strait to the central

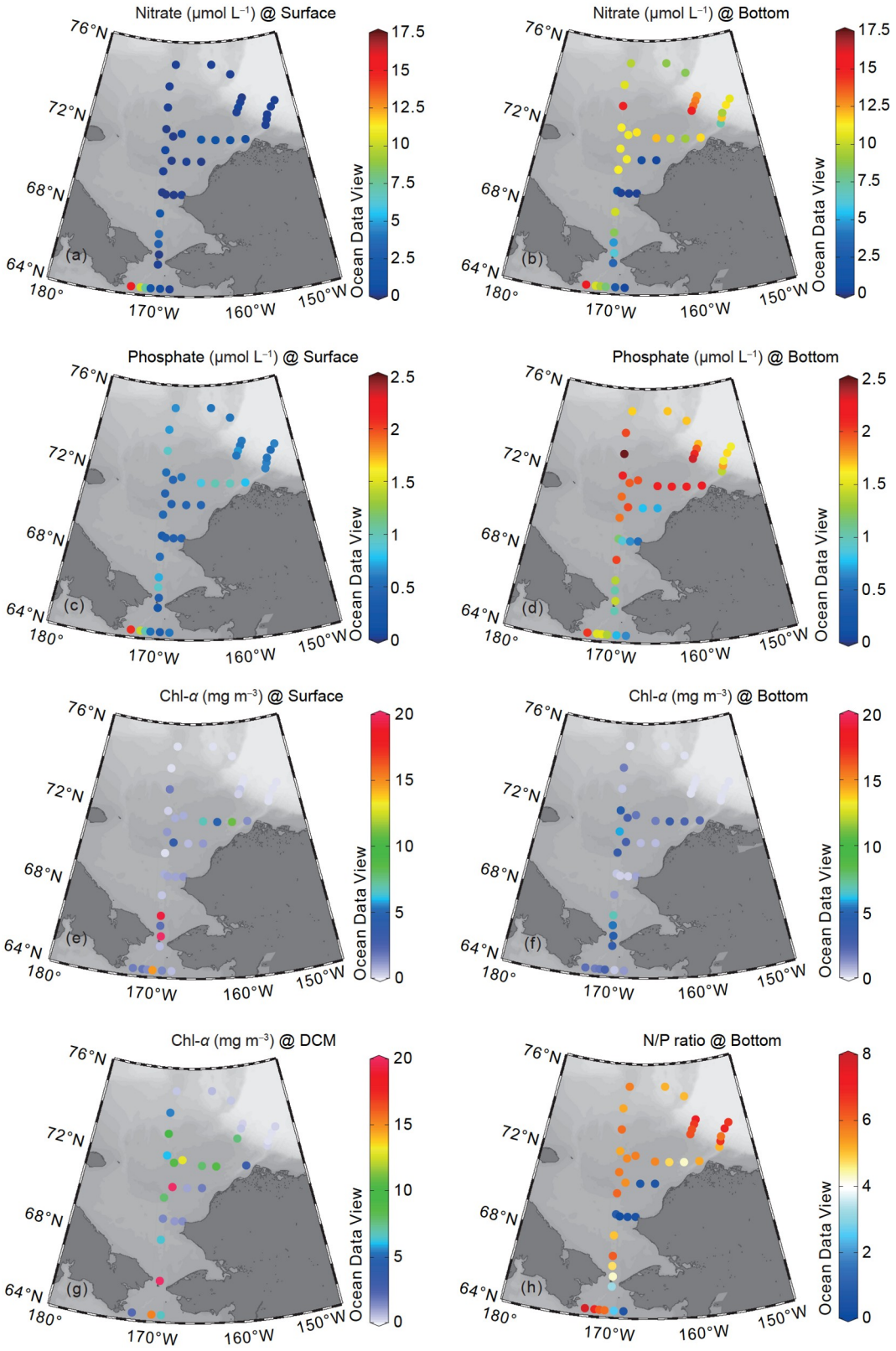

Figure 3 Maps of water column biogeochemical parameters on the Bering-Chukchi shelf, August–September 2008: (a) surface $[NO_3^-]$, (b) bottom $[NO_3^-]$, (c) surface $[PO_4^{3-}]$, (d) bottom $[PO_4^{3-}]$, (e) surface [Chl-*a*], (f) bottom [Chl-*a*], (g) maximum [Chl-*a*] of the water column, and (h) bottom N/P ratio. The bottom layer represents the deepest sampling depth on the shelf (<100 m water depth), while those are samples at 100 m depth on the slope and basin area (>100 m water depth). DCM means depth of chlorophyll maximum.

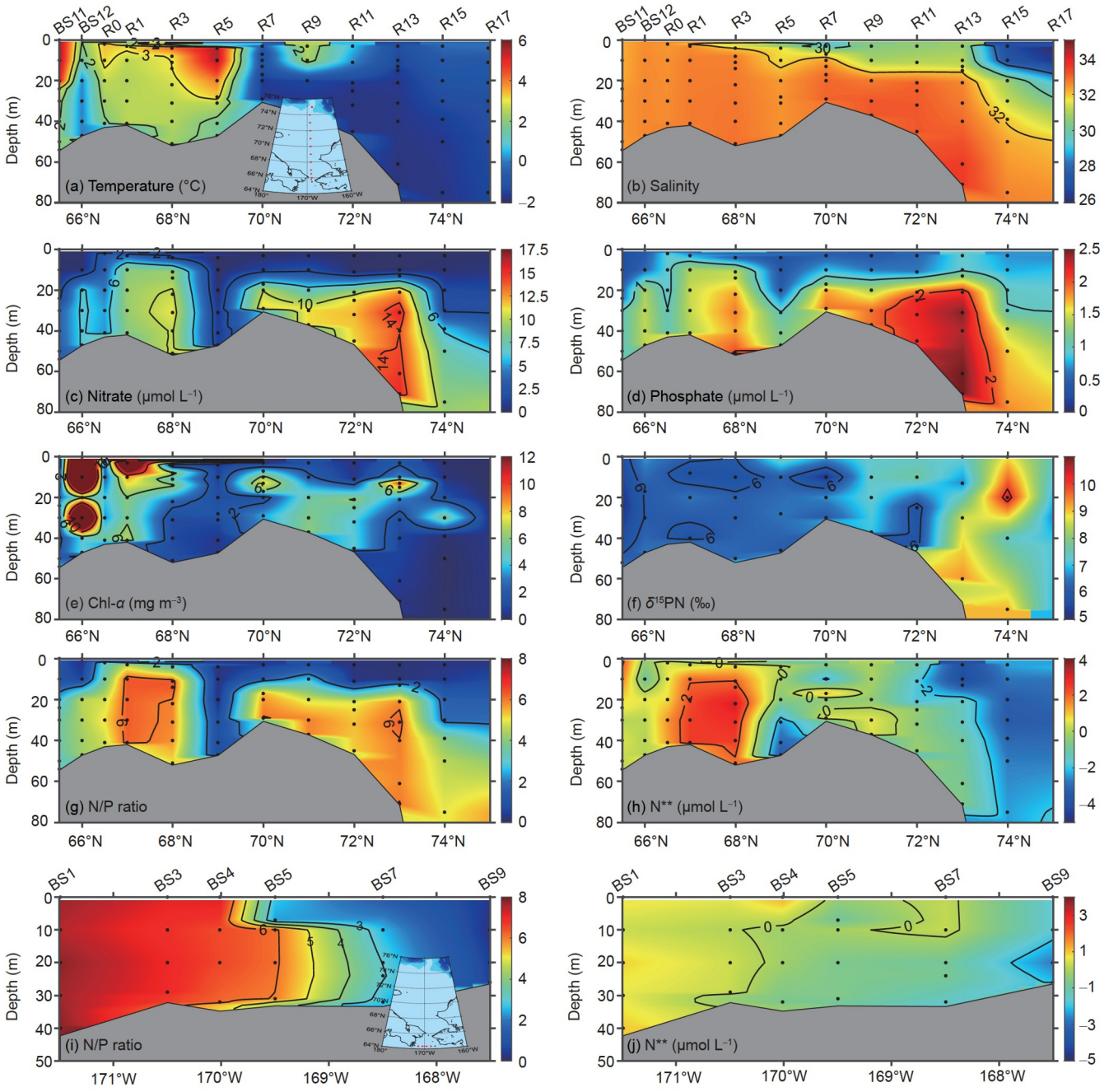

Figure 4 Vertical sections of water column properties along meridional transect *R* on the Bering-Chukchi shelf (panels (a)–(f)): (a) Temperature, (b) Salinity, (c) $[NO_3^-]$, (d) $[PO_4^{3-}]$, (e) [Chl-*a*], (f) δ^{15}PN, (g) N/P ratio, and (h) N**, and zonal transect BS just south of the Bering Strait (panels (i)–(j)): (i) N/P ratio, and (j) N** (N**=$([NO_3^-]+[NO_2^-])-8.8\times[PO_4^{3-}]+2.98$), August–September 2008. For transect locations, see the maps in panel (a) and panel (g).

Chukchi Sea (72°N). The northern Chukchi shelf was characterized by significantly heavier δ^{15}PN (7.0‰ to 10.0‰), particularly in the bottom layer between 73°N and 74°N.

Values of $\delta^{15}N_{sediment}$ across the Chukchi shelf (Figure 5c) ranged from 5.0‰ to 9.2‰, with an average value of 7.3 ±0.8‰. Values increased poleward, with $\delta^{15}N_{sediment}$ and latitude being significantly correlated (r=0.89, p<0.01, n=14). The lightest $\delta^{15}N_{sediment}$ values (5.7‰ to 6.8‰) were observed in the Bering Strait and on the adjacent southern Chukchi shelf. Intermediate values (7.0‰ to 7.9‰) were observed on the central shelf, and the heaviest values (9.2‰) were seen on the northern shelf.

3.3.2 *Temporal variability of δ^{15}PN and PN flux in sinking particles*

The PN flux and δ^{15}PN of sinking particles sampled at 870 m on the Chukchi slope (Figure 1) from August 2008 through September 2009 is shown in Figure 6. During late summer

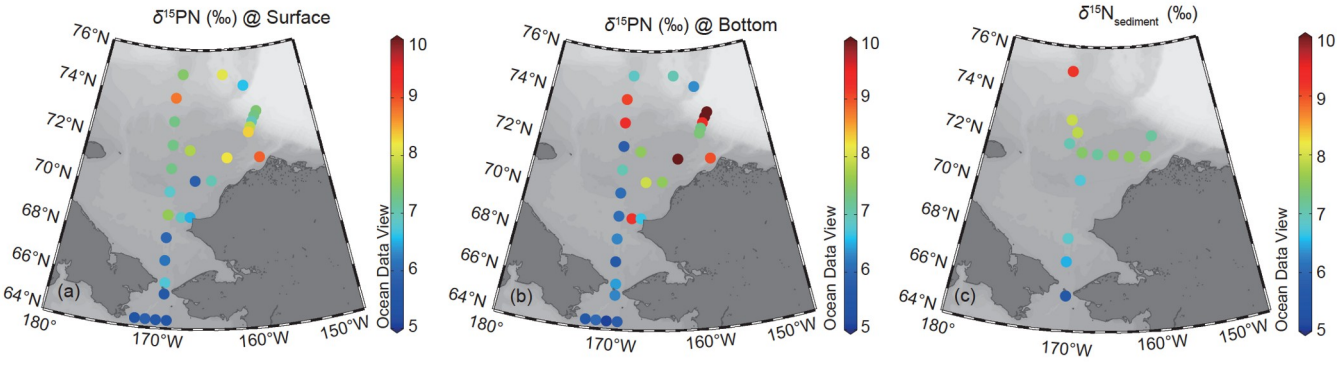

Figure 5 Maps of biogeochemical parameter distributions on the Bering-Chukchi shelf: (a) surface water δ^{15}PN, (b) bottom water δ^{15}PN, and (c) $\delta^{15}N_{sediment}$. The water column was sampled in 2008, and the surface sediments were sampled in 2003.

2008 (first half of August), δ^{15}PN was rather high (9.3‰), coincident with high PN flux (2.04 mg m^{-2} d^{-1}), high PAR, high SST, and the thinning of sea ice. With the disappearance of sea ice, the δ^{15}PN and PN flux declined to 7.6‰±0.6‰ (6.8‰ to 8.4‰) and 0.52±0.21 mg m^{-2} d^{-1} (0.29 to 0.86 mg m^{-2} d^{-1}) from mid-August to the end of October. At the beginning of November, sea ice re-formed rapidly, and δ^{15}PN thereafter maintained at lighter levels (6.7‰ to 8.6‰, with an average of 7.9‰±0.6‰) with lower PN flux (0.13 to 0.62 mg m^{-2} d^{-1}, with an average of 0.29±0.20 mg m^{-2} d^{-1}) during winter time, except for the extremely high δ^{15}PN value (13.9‰) in April 2009. During the second summer of observations, δ^{15}PN and PN fluxes were again high, with an average of 9.4‰±0.9‰ (7.9‰ to 10.8‰) and 1.61±1.27 mg m^{-2} d^{-1} (0.16 to 4.27 mg m^{-2} d^{-1}), respectively. In comparison, the δ^{15}PN values in the summer of 2009 were slightly higher than in the preceding summer (independent-Samples *T* test, $p<0.05$).

4. Discussion

4.1 Biological utilization of NO_3^- and vertical export of PN

Several lines of evidence indicate warm-season utilization of Chukchi Sea NO_3^- by phytoplankton and subsequent PN export to the seafloor. During the August–September 2008 period of observation, Pacific throughflow waters in the Chukchi Sea exhibited a nitrate-depleted upper layer, with the nitracline deepening from about 5 m in the Bering Strait to about 30 m in the northern Chukchi Sea (Figure 4c). Over that same area, the δ^{15}PN showed poleward enrichment (Figure 4f), consistent with the deepening nitracline. Within the upper water column (30 m) of the northward section R, δ^{15}PN and $\ln([NO_3^-])$ fit a linear regression relationship ($r=-0.80$, $p<0.01$), suggesting that the increased δ^{15}PN of suspended particles is an assimilation signature of phytoplankton. Similarly, the $\delta^{15}N_{sediment}$, a good sedimentary proxy of nitrate utilization in upper waters, also showed poleward enrichment (Figure 5c), and positive correlation with those of weighted δ^{15}PN in the upper water column ($r=0.80$, $p<0.01$). Although there were five years sampling gap between sediment samples and water column samples, the sedimentation rate is slower than 1 mm yr^{-1} in the Chukchi Sea (Vologina et al., 2018), and these poleward distribution trends were also consistent with the trends reported by previous studies (Codispoti et al., 2009; Nishino et al., 2016).

At the Bering Strait, the entry point for Pacific inflow into the Arctic basin, maximum surface [Chl-*a*] was observed (22.4 mg m^{-3}), along with relatively high $[NO_3^-]$ and light δ^{15}PN (Figure 4c–4f). On the central and northern Chukchi shelf (i.e., farther along the water's a northward path), surface [Chl-*a*] declined to <1.0 mg m^{-3} and subsurface maxima appeared (Figure 4e). The surface $[NO_3^-]$ declined, and δ^{15}PN throughout the water column reflected enrichment in heavier isotopes (Figure 4f). Although the occurrence of upwelling in the middle of the shelf (72°N–74°N), the subsurface water also originated from PWW, the same nitrogen source compared to other regions. Based on ^{234}Th/^{238}U disequilibrium, Yu et al. (2012) observed that the average POC export flux was about 354±276 mg m^{-2} d^{-1} on the Chukchi shelf during our 2008 cruises. Assuming the C/N ratios of the sinking particles were consistent with Redfield ratio (6.6), about 53.6±41.8 mg m^{-2} d^{-1} of PN was exported to the benthos. These observations are all consistent with the conclusion that continuous assimilation of nitrate by phytoplankton was the main reason for the observed northward $[NO_3^-]$ depletion in summer.

Light availability, which is controlled in part by sea ice conditions (e.g., areal coverage and thickness), exerts a key control on primary production and thus nitrate utilization (Tremblay et al., 2015). As shown in Figure 6, the PN flux and δ^{15}PN of sinking particles at station M01 exhibited dramatic seasonal variability in association with fluctuating environmental conditions at the sea surface (e.g., PAR, SST, sea ice concentration, and Chl-*a*). Highly positive δ^{15}PN values (9.4‰±0.9‰) and high PN flux (1.38±1.30 mg m^{-2} d^{-1})

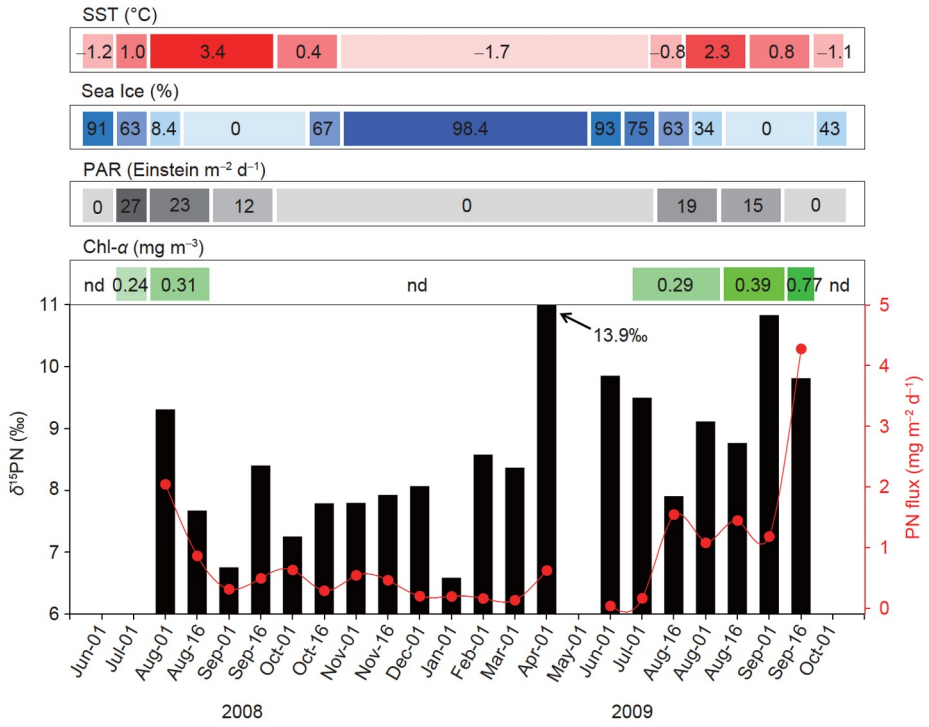

Figure 6 Temporal trends at mooring station M01, August 2008–September 2009: particulate nitrogen (PN) sinking flux (red dots) at 870 m depth and corresponding δ^{15}PN (black bars). The horizontal bars at the top of the panel show weekly sea surface temperature (SST), sea ice concentration, photosynthetically available radiation (PAR), and surface Chl-*a* data. In the Chl-*a* panel, nd represents no data.

in sinking particles were observed from June to mid-September 2009, a time of high incident solar radiation and SST, as a result, little to no sea ice and high surface Chl-*a*. These extremely high δ^{15}PN values and high phytoplankton biomass are indicative of high utilization of nitrate during the growing season.

It is notable that within the summer of 2008, only the first half of August exhibited a highly positive δ^{15}PN value with high PN flux (2.04 mg m^{-2} d^{-1}). For the remainder of this summer, the flux ranged from only 0.31 to 0.86 mg m^{-2} d^{-1}, with light δ^{15}PN values (7.6‰±0.6‰). This temporal pattern suggests that upper-ocean NO_3^- may have been completely depleted by consumption associated with a phytoplankton bloom (high PN flux) in early August 2008 when the sea ice concentration was low (8.4%). The subsequent open water period was characterized by low PN flux and light δ^{15}PN, probably due to the exhausting of nitrate but increasing of adsorbed inorganic nitrogen in the PN (Schubert and Calvert, 2001).

We attribute the high nitrate utilization and nitrate-depleted state of Chukchi Sea waters to the spatiotemporal coupling of biological nutrient assimilation and particulate export to the deep ocean or benthos.

4.2 Seasonal N and P consumption

For each 2008 station, consumption of NO_3^- and PO_4^{3-} was estimated from their seasonal deficits (i.e., differences in concentrations between the cold- and warm-season waters). Using the average PWW nutrient concentrations (Table 1) to represent conditions at the start of the growing season yields an average depth-integrated (0–100 m) Chukchi shelf and slope deficit of 437±205 mmol m^{-2} for NO_3^- (Figure 7a) and 52±24 mmol m^{-2} for PO_4^{3-} (Figure 7b). At station M01, the estimated NO_3^- deficit was 758.4 mmol m^{-2} and the PO_4^{3-} deficit was 87.1 mmol m^{-2}. These 2008 estimates are similar to the Chukchi shelf deficits calculated by Mills et al. (2015) for the years 2010 (588±250 mmol m^{-2} for NO_3^- and 52±24 mmol m^{-2} for PO_4^{3-}) and 2011 (930±450 mmol m^{-2} for NO_3^- and 82±38 mmol m^{-2} for PO_4^{3-}).

Notably, high consumption of NO_3^- and PO_4^{3-} was observed near the Central Channel (69°N), Barrow Canyon, and northern Chukchi shelf break (74°N–75°N) (Figure 7a, 7b). These areas have been previously documented as areas of high primary productivity, both during our sampling period (Coupel et al., 2015) and during earlier summertime studies (Hill and Cota, 2005). The Central Channel and Barrow Canyon areas experience longer growing seasons than other parts of the shelf due to early ice melt (induced by the springtime warming of relatively warm ACW water) and occasional polynya formation (due to local winds) (Itoh et al., 2015).

At station M01, the time series of sinking particle flux

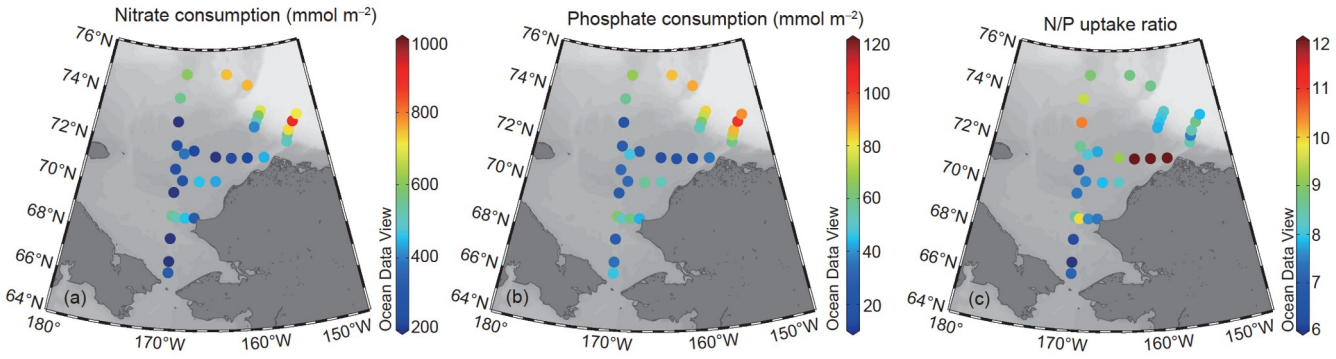

Figure 7 Maps showing depth-integrated (0–100 m) nutrient parameters across the Chukchi shelf and slope for the 2008 growing season: (a) NO_3^- consumption, (b) PO_4^{3-} consumption, and (c) N/P uptake ratios.

(Figure 6) can be used to estimate the export of PN from the upper ocean over the course of the 2008 growing season. In an ideal steady-state environment, the export PN flux should theoretically equal the NO_3^- consumption. The aggregated (cumulative) PN trap flux from April to mid-August was 120.5±26.4 mmol m^{-2}. According to (the inverse solution of) the function given by Martin et al. (1987) for the vertical attenuation of PN in the open ocean water column (i.e., $F_z=F_{100}(z/100)^{-0.988}$, where F_z is the flux at any depth, F_{100} is the flux at 100 m depth, and z is depth in meters), the total estimated PN export flux at 100 m during our study would have been 1021.9±224.1 mmol m^{-2}. This estimate is significantly greater than the estimated nitrate consumption at this station (758.4 mmol m^{-2}).

The estimated PN export flux could be an overestimate if some particles arrived at the sediment trap via lateral advection rather than vertical sinking. The consistent seasonal variation of the PN trap fluxes with the seasonal variations of SST, solar radiation, sea ice coverage and surface Chl-*a* (Figure 6) qualitatively indicated coupling between upper ocean primary production and PN fluxes at the sediment trap. So did the seasonal variations of brassicasterol, dinosterol, and cholesterol (proxies of upper-layer plankton production) in the trap samples, with the July–September samples containing more of these compounds than the cold-season samples (Bai et al., 2018). Also, the C/N ratio (5.7 to 8.5, with an average of 7.5±0.6) suggested that the sinking particle fluxes are mainly of marine origin (Bai et al., 2018). However, the existence of an appreciable PN flux during the dark, iced-over cold season did suggest some lateral input. So did previous work in the Canada Basin. Radioactive carbon isotope ($\Delta^{14}C$) values of particulate organic carbon previously collected in Canada Basin sediment traps (Honjo et al., 2010; Hwang et al., 2008) suggested that the organic matter collected at 120 m was mostly autochthonous whereas that collected at 3067 m was mostly aged and allochthonous. At our intermediate depth of 870 m, then, lateral transport could have carried some particles into the station M01 collection bottles.

If we assume that lateral inputs are constant year-round, we can subtract the wintertime (December 2008 to March 2009) average PN flux from the original estimate of growing-season flux to yield a corrected growing-season flux at station M01. By this method, the estimated vertical PN flux at 100 m would have been 903.9±215.6 mmol m^{-2}, which is a closer match to the estimated NO_3^- growing-season deficit of 758.4 mmol m^{-2}.

4.3 N/P uptake and preferential removal of N from Pacific throughflow

The phytoplankton N/P uptake ratio of the 2008 Chukchi Sea growing season (Figure 7c) averaged 8.8±2.27, which was significantly less than the canonical Redfield ratio of 16. This deviation was consistent with the results of previous Arctic studies, which found uptake ratios of approximately 9.2 and 12.0 (Chukchi shelf), 6 (Baffin Bay), 4 (Beaufort Sea), and 8 (Bering Sea) (Mills et al., 2015; Tremblay et al., 2015) as well a particle N/P ratio of 10 (Chukchi Sea) (Piper et al., 2016).

The physiological responses of phytoplankton to different growing conditions may help to explain these deviations of stoichiometry from the Redfield utilization ratios. Under optimal growing conditions (e.g., adequate light and nutrients, low temperature), phytoplankton may produce generally more ribosomal RNA and nucleic acids (low N/P) in association with high growth rates. Under suboptimal (warm temperature, nutrient-depleted, or otherwise growth-limiting conditions), the cells would contain more protein (high N/P) (Elser et al., 1996). The Arctic spring combination of abundant nutrients and abundant light provides optimal growing conditions, first at the sea surface and then later, as surface nutrients are depleted, in subsurface waters—hence favoring low N/P uptake and efficient vertical export, as observed during the 2008 growing season.

Phytoplankton community composition may also play a

role in determining N/P uptake ratios. Global patterns of particulate elemental stoichiometry show low N/P in high-latitude regions dominated by diatoms but high N/P in oligotrophic subtropical gyres dominated by cyanobacteria (Martiny et al., 2013). During Chukchi shelf growing seasons, diatoms can account for nearly 60% of the total biomass (according to taxonomic enumeration) or even 70% (according to pigment analysis) (Coupel et al., 2012). Hence, the low Chukchi N/P uptake ratios may be related to the overwhelming dominance of diatoms during the summer growing season.

The Chukchi shelf N/P uptake ratio of ~9 is low compared to the Redfield ratio but still about twice the average N/P measured in the Pacific inflow waters. Along the zonal BS transect south of the Bering Strait (Figure 4i), the average N/P was only 4.8±2.69; for PWW on the Chukchi Shelf, the average N/P was 5.7±0.42 (Figures 2b, 3h and 4i). These low inflow ratios reflected the loss of fixed nitrogen from the bottom water on the Bering shelf due to coupled sedimentary nitrification-denitrification processes (Granger et al., 2011). However, according to the N^{**} value (−0.93±1.55 μmol L^{-1}, Figure 4h and 4j) and light $\delta^{15}NO_3^-$ of the PWW (5.7‰±0.9‰, Granger et al., 2011), we could basically exclude the effect of microbial denitrification on the N/P ratio in the Chukchi Sea waters.

According to our calculations of nutrient consumption across the entire Chukchi Sea, about 260×10^9 mol N yr^{-1} and 30.9×10^9 mol P yr^{-1} were utilized for NO_3^- and PO_4^{3-} phytoplankton uptake during the 2008 growing season. If uptake had instead followed the N/P ratio of the source water (i.e., a ratio of 4.8 to 5.7 instead of 8.8, with no change in PO_4^{3-} uptake), then the 2008 NO_3^- uptake would have been only about half of that observed. In other words, an additional 83.9×10^9 to 111.7×10^9 mol N yr^{-1} of NO_3^- should have remained in the upper water column at the end of the growing season.

As estimated by previous studies, about 20%–82% of the primary production was efficiently exported to the seafloor during the Chukchi warm season (Moran et al., 2005; Yu et al., 2012; Zhang R et al., 2015; O'Daly et al., 2020), consumed NO_3^- should be quickly transformed to sinking PN that is subsequently export to the shallow shelf. The extra N consumption (relative to P) therefore represents a significant removal of N from upper Arctic waters. Whether would sea ice formation induced mixing to reintroduce remineralized N into the water column? By a two-layer mode and the Fick's first law of diffusion, Zhang H et al. (2015) estimated that the diffusive fluxes of nitrate in the middle of Chukchi Sea shelf were 0.117 mmol m^{-2} d^{-1}. Assuming the duration of sea ice lasts for 180 d, the total amount of the exported nitrate back to the water column is 21.06 mmol m^{-2}. The nitrate stock during this period is 610 mmol m^{-2}, which is calculated by the average nitrate concentration of PWW (Table 1) multiplying by the average Chukchi Sea depth (50 m). Thus, the remineralized N accounts for about 3.5% of the N stock. Additionally, the nitrate concentration of PWW is comparable with that of the Anadyr Water, indicating that the Pacific inflow is the main source of nutrient to the Chukchi Shelf during this unproductive season. On the seasonal timescale, the biological removal of N in summer and the water mixing in winter are de-coupled processes, and the well mixed PWW usually intrudes into the subsurface (>100 m) of Canada Basin, while the surface mixed layer depth is about 50 m (Timmermans and Marshall, 2020). Hence, even if part of the sinking PN flux gets remineralized at the benthic boundary layer after the growing season, the regenerated nutrients hardly return to the upper layer to fuel phytoplankton growth again due to strong stratification with a freshening trend in the high latitude area.

With the annual marine denitrification rate for the Chukchi Sea estimated at about 214×10^9 mol N yr^{-1} (Chang and Devol, 2009), the rate of extra N consumption by the biological pump within the Chukchi Sea is approximately 39% to 52% of denitrification rate. Although the nitrogen removal caused by the biological pump process is not the ultimate nitrogen sink like denitrification, it has been overlooked that it happens before denitrification and pre-plays an important role on the nitrogen cycle in Arctic Ocean. Additionally, its negative effect on marine ecosystems is probably significant in a foreseeable future due to lower nitrogen availability in the euphotic zone.

The preferential removal of N from the Chukchi water column (relative to P) by the biological pump thus exacerbates the condition of Arctic N limitation, with implications for primary production and biogeochemical cycling across the pan Arctic Ocean and beyond. For example, Yamamoto-Kawai et al. (2006) estimated that the 2×10^{10} mol yr^{-1} excess PO_4^{3-} that results from Pacific inflow (already depleted NO_3^- relative to PO_4^{3-}) and Arctic sedimentary denitrification (further reducing the ratio of NO_3^- to PO_4^{3-}) accounts for 16% or more of the nitrogen fixation in the North Atlantic Ocean. Our work indicates that west Arctic phytoplankton utilization of nutrients at ratios greater than the N/P ratio of the inflowing source water may also contribute to excess PO_4^{3-} in the Arctic and North Atlantic oceans. To sum up the above discussion, a conceptual scheme of the nitrogen deficit induced by the biological carbon pump in the Chukchi Sea is proposed in Figure 8. With ongoing rapid Arctic Ocean change (e.g., sea ice retreat, a longer phytoplankton growing season, and increasing Chukchi Sea primary production), the combined effect of biological pump processes and sedimentary denitrification will likely exert an increasingly important influence on nitrogen deficit dynamics and marine biogeochemical cycling in the Arctic and adjacent North Atlantic oceans.

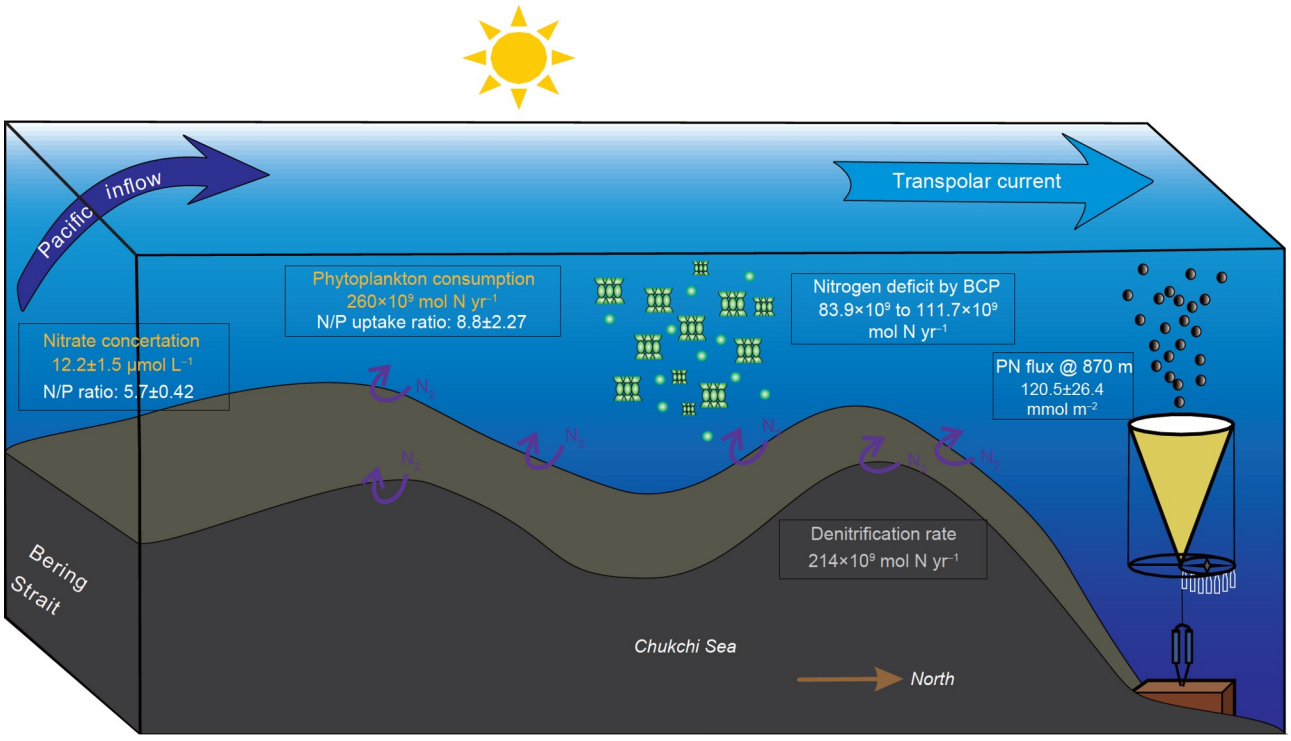

Figure 8 Conceptual scheme of the nitrogen deficit induced by the biological carbon pump (BCP) in the Chukchi Sea. Through the Bering Strait, the Pacific inflow serves the main nutrient source to the Chukchi Sea with a low N/P ratio, the biological carbon pump consumes the nitrate with a higher N/P ratio than that of the source water. As a result, the BCP could also cause nitrogen deficit due to extra nitrate consume. The particulate nitrogen (PN) flux at 870 m collected by sediment trap and denitrification rate at the sediment-water interface (Chang and Devol, 2009) were also showed in the plot.

5. Conclusions

Based on analyses of west Arctic sediments, water column constituents, suspended and sinking particles, we demonstrate that a phytoplankton N/P requirement higher than the N/P ratio of the inflowing source water in conjunction with efficient nitrogen export to the seabed significantly skews the nutrient properties of Pacific inflow water as it crosses the Chukchi Sea, thus further decreasing an already low N/P ratio. This biological pump effect has not been previously characterized. During the 2008 growing season, extra N (relative to P) was consumed as Pacific inflow waters crossed the Chukchi shelf, thereby leading to increasingly severe N limitation and additional excess P in the upper waters of the Arctic Ocean. In other words, biological uptake and export significantly enhance N removal from the upper Arctic water column every summer, which should also be considered when preoccupant opinions regard sedimentary denitrification as the major reason for N deficit in the Pacific Arctic.

Acknowledgements *We thank the captain and crew of the R/V Xuelong icebreaker for their assistance with sample collection during the two cruises. We thank Professor J. P. Zhao (Ocean University of China) and the physical oceanography teams for their acquisition and sharing of the hydrographic (CTD) data. We also thank F. J. Chen (Guang Dong Ocean University) for detecting $\delta^{15}N$ of sinking particles samples. We thank Reiner Schlitzer and his group for sharing the Ocean Data View graphics program (http://www.odv.awi.de). We thank Tonya Clayton for her professional help with English language editing. This work was supported by the National Natural Science Foundation of China (Grant Nos. 41003036 & 41941013), the Chinese National Arctic Research Expedition Project (CHINARE), the Cai Yuanpei Program, and the ICAR Project (China Scholarship Council).*

References

Arrigo K R, van Dijken G L. 2015. Continued increases in Arctic Ocean primary production. Prog Oceanogr, 136: 60–70

Bai Y, Sicre M A, Chen J, Klein V, Jin H, Ren J, Li H, Xue B, Ji Z, Zhuang Y, Zhao M. 2018. Seasonal and spatial variability of sea ice and phytoplankton biomarker flux in the Chukchi Sea (western Arctic Ocean). Prog Oceanogr, 171: 22–37

Beszczynska-Möller A, Woodgate R, Lee C, Melling H, Karcher M. 2011. A synthesis of exchanges through the main oceanic gateways to the Arctic Ocean. Oceanography, 24: 82–99

Brown Z W, Casciotti K L, Pickart R S, Swift J H, Arrigo K R. 2015. Aspects of the marine nitrogen cycle of the Chukchi Sea shelf and Canada Basin. Deep-Sea Res Part II-Top Stud Oceanogr, 118: 73–87

Chang B X, Devol A H. 2009. Seasonal and spatial patterns of sedimentary denitrification rates in the Chukchi sea. Deep-Sea Res Part II-Top Stud Oceanogr, 56: 1339–1350

Codispoti L A, Flagg C, Kelly V, Swift J H. 2005. Hydrographic conditions during the 2002 SBI process experiments. Deep-Sea Res Part II-Top Stud Oceanogr, 52: 3199–3226

Codispoti L A, Flagg C N, Swift J H. 2009. Hydrographic conditions during the 2004 SBI process experiments. Deep-Sea Res Part II-Top Stud Oceanogr, 56: 1144–1163

Codispoti L A, Kelly V, Thessen A, Matrai P, Suttles S, Hill V, Steele M, Light B. 2013. Synthesis of primary production in the Arctic Ocean: III. Nitrate and phosphate based estimates of net community production. Prog Oceanogr, 110: 126–150

Cooper L W, Cota G F, Pomeroy L R, Grebmeier J M, Whitledge T E.

1999. Modification of NO, PO, and NO/PO during flow across the Bering and Chukchi shelves: Implications for use as Arctic water mass tracers. J Geophys Res, 104: 7827–7836
Coupel P, Jin H Y, Joo M, Horner R, Bouvet H A, Sicre M A, Gascard J C, Chen J F, Garçon V, Ruiz-Pino D. 2012. Phytoplankton distribution in unusually low sea ice cover over the Pacific Arctic. Biogeosciences, 9: 4835–4850
Coupel P, Ruiz-Pino D, Sicre M A, Chen J F, Lee S H, Schiffrine N, Li H L, Gascard J C. 2015. The impact of freshening on phytoplankton production in the Pacific Arctic Ocean. Prog Oceanogr, 131: 113–125
Devol A H, Codispoti L A, Christensen J P. 1997. Summer and winter denitrification rates in western Arctic shelf sediments. Cont Shelf Res, 17: 1029–1050
Elser J J, Dobberfuhl D R, MacKay N A, Schampel J H. 1996. Organism size, life history, and N:P stoichiometry. Bioscience, 46: 674–684
Granger J, Prokopenko M G, Sigman D M, Mordy C W, Morse Z M, Morales L V, Sambrotto R N, Plessen B. 2011. Coupled nitrification-denitrification in sediment of the eastern Bering Sea shelf leads to ^{15}N enrichment of fixed N in shelf waters. J Geophys Res, 116: C11006
Grasshoff K, Kremling K, Manfred E. 1999. Methods of Seawater Analysis. New York: Wiley-VCH. 600
Grebmeier J M, Bluhm B A, Cooper L W, Danielson S L, Arrigo K R, Blanchard A L, Clarke J T, Day R H, Frey K E, Gradinger R R, Kędra M, Konar B, Kuletz K J, Lee S H, Lovvorn J R, Norcross B L, Okkonen S R. 2015. Ecosystem characteristics and processes facilitating persistent macrobenthic biomass hotspots and associated benthivory in the Pacific Arctic. Prog Oceanogr, 136: 92–114
Hill V, Ardyna M, Lee S H, Varela D E. 2018. Decadal trends in phytoplankton production in the Pacific Arctic Region from 1950 to 2012. Deep-Sea Res Part II-Top Stud Oceanogr, 152: 82–94
Hill V, Cota G. 2005. Spatial patterns of primary production on the shelf, slope and basin of the Western Arctic in 2002. Deep-Sea Res Part II-Top Stud Oceanogr, 52: 3344–3354
Holm-Hansen O, Lorenzen C J, Holmes R W, Strickland J D H. 1965. Fluorometric determination of chlorophyll. ICES J Mar Sci, 30: 3–15
Honjo S, Krishfield R A, Eglinton T I, Manganini S J, Kemp J N, Doherty K, Hwang J, McKee T K, Takizawa T. 2010. Biological pump processes in the cryopelagic and hemipelagic Arctic Ocean: Canada Basin and Chukchi Rise. Prog Oceanogr, 85: 137–170
Hwang J, Eglinton T I, Krishfield R A, Manganini S J, Honjo S. 2008. Lateral organic carbon supply to the deep Canada Basin. Geophys Res Lett, 35: 58–70
Itoh M, Pickart R S, Kikuchi T, Fukamachi Y, Ohshima K I, Simizu D, Arrigo K R, Vagle S, He J, Ashjian C, Mathis J T, Nishino S, Nobre C. 2015. Water properties, heat and volume fluxes of Pacific water in Barrow Canyon during summer 2010. Deep-Sea Res Part I-Oceanogr Res Pap, 102: 43–54
Knap A, Micheals A, Close A, Ducklow H, Dickson A. 1996. Protocols for the Joint Global Ocean Flux (JGOFS) Core measurements Report no. 19, IOC Manuals and guides, UNESCO, 29
Martin J H, Knauer G A, Karl D M, Broenkow W W. 1987. VERTEX: Carbon cycling in the northeast Pacific. Deep Sea Res Part A Oceanogr Res Pap, 34: 267–285
Martiny A C, Pham C T A, Primeau F W, Vrugt J A, Moore J K, Levin S A, Lomas M W. 2013. Strong latitudinal patterns in the elemental ratios of marine plankton and organic matter. Nat Geosci, 6: 279–283
McLaughlin F A, Carmack E C, Macdonald R W, Melling H, Swift J H, Wheeler P A, Sherr B F, Sherr E B. 2004. The joint roles of Pacific and Atlantic-origin waters in the Canada Basin, 1997–1998. Deep-Sea Res Part I-Oceanogr Res Pap, 51: 107–128
Mills M M, Brown Z W, Lowry K E, van Dijken G L, Becker S, Pal S, Benitez-Nelson C R, Downer M M, Strong A L, Swift J H, Pickart R S, Arrigo K R. 2015. Impacts of low phytoplankton NO3−:PO43− utilization ratios over the Chukchi Shelf, Arctic Ocean. Deep-Sea Res Part II-Top Stud Oceanogr, 118: 105–121
Moran S B, Kelly R P, Hagstrom K, Smith J N, Grebmeier J M, Cooper L W, Cota G F, Walsh J J, Bates N R, Hansell D A, Maslowski W, Nelson R P, Mulsow S. 2005. Seasonal changes in POC export flux in the Chukchi Sea and implications for water column-benthic coupling in Arctic shelves. Deep-Sea Res Part II-Top Stud Oceanogr, 52: 3427–3451
Nishino S, Kikuchi T, Fujiwara A, Hirawake T, Aoyama M. 2016. Water mass characteristics and their temporal changes in a biological hotspot in the southern Chukchi Sea. Biogeosciences, 13: 2563–2578
O'Daly S H, Danielson S L, Hardy S M, Hopcroft R R, Lalande C, Stockwell D A, McDonnell A M P. 2020. Extraordinary carbon fluxes on the shallow pacific arctic shelf during a remarkably warm and low sea ice period. Front Mar Sci, 7: 548931
Piper M M, Benitez-Nelson C R, Frey K E, Mills M M, Pal S. 2016. Dissolved and particulate phosphorus distributions and elemental stoichiometry throughout the Chukchi Sea. Deep-Sea Res Part II-Top Stud Oceanogr, 130: 76–87
Schubert C J, Calvert S E. 2001. Nitrogen and carbon isotopic composition of marine and terrestrial organic matter in Arctic Ocean sediments: Implications for nutrient utilization and organic matter composition. Deep-Sea Res Part I-Oceanogr Res Pap, 48: 789–810
Steele M, Morison J, Ermold W, Rigor I, Ortmeyer M, Shimada K. 2004. Circulation of summer Pacific halocline water in the Arctic Ocean. J Geophys Res, 109: C02027
Timmermans M L, Marshall J. 2020. Understanding Arctic Ocean circulation: A review of ocean dynamics in a changing climate. J Geophys Res-Oceans, 125: e2018JC014378
Torres-Valdés S, Tsubouchi T, Bacon S, Naveira-Garabato A C, Sanders R, McLaughlin F A, Petrie B, Kattner G, Azetsu-Scott K, Whitledge T E. 2013. Export of nutrients from the Arctic Ocean. J Geophys Res-Oceans, 118: 1625–1644
Tremblay J É, Anderson L G, Matrai P, Coupel P, Bélanger S, Michel C, Reigstad M. 2015. Global and regional drivers of nutrient supply, primary production and CO_2 drawdown in the changing Arctic Ocean. Prog Oceanogr, 139: 171–196
Vologina E G, Kalugin I A, Dar'in A V, Astakhov A S, Sturm M, Chernyaeva G P, Kulagina N V, Kolesnik A N. 2018. Late holocene sedimentation in active geological structures of the Chukchi Sea. Geodin tektonofiz, 9: 199–219
Walsh J J, McRoy C P, Coachman L K, Goering J J, Nihoul J J, Whitledge T E, Blackburn T H, Parker P L, Wirick C D, Shuert P G, Grebmeier J M, Springer A M, Tripp R D, Hansell D A, Djenidi S, Deleersnijder E, Henriksen K, Lund B A, Andersen P, Müller-Karger F E, Dean K. 1989. Carbon and nitrogen cycling within the Bering/Chukchi Seas: Source regions for organic matter effecting AOU demands of the Arctic Ocean. Prog Oceanogr, 22: 277–359
Weingartner T, Aagaard K, Woodgate R, Danielson S, Sasaki Y, Cavalieri D. 2005. Circulation on the north central Chukchi Sea shelf. Deep-Sea Res Part II-Top Stud Oceanogr, 52: 3150–3174
Woodgate R A. 2018. Increases in the Pacific inflow to the Arctic from 1990 to 2015, and insights into seasonal trends and driving mechanisms from year-round Bering Strait mooring data. Prog Oceanogr, 160: 124–154
Yamamoto-Kawai M, Carmack E, McLaughlin F. 2006. Nitrogen balance and Arctic throughflow. Nature, 443: 43
Yu W, He J, Li Y, Lin W, Chen L. 2012. Particulate organic carbon export fluxes and validation of steady state model of ^{234}Th export in the Chukchi Sea. Deep-Sea Res Part II-Top Stud Oceanogr, 81-84: 63–71
Zhang H, Zhuang Y, Zhu Q, Li H, Liu X, Chen F, Lu Y, Chen J. 2015. Estimation of nutrients flux of water-sediment interface in the Chukchi Sea, the western Arctic Ocean (in Chinese). Acta Oceanol Sin, 37: 155–164
Zhang R, Chen M, Ma Q, Cao J, Qiu Y. 2015. Insights into the coupling of upper ocean-benthic carbon dynamics in the western Arctic Ocean from an isotopic (^{13}C, ^{234}Th) perspective. Acta Oceanol Sin, 34: 26–33

(Responsible editor: Zhimin JIAN)